Rotational study of the NH3–CO complex: Millimeter-wave measurements and ab initio calculations

L. A. Surin, A. Potapov, A. A. Dolgov, I. V. Tarabukin, V. A. Panfilov, S. Schlemmer, Y. N. Kalugina, A. Faure, and A. van der Avoird

Citation: The Journal of Chemical Physics **142**, 114308 (2015); doi: 10.1063/1.4915119
View online: http://dx.doi.org/10.1063/1.4915119
View Table of Contents: http://scitation.aip.org/content/aip/journal/jcp/142/11?ver=pdfcov
Published by the AIP Publishing

Rotational study of the NH_3–CO complex: Millimeter-wave measurements and *ab initio* calculations

L. A. Surin,[1,2,a)] A. Potapov,[1] A. A. Dolgov,[2] I. V. Tarabukin,[2] V. A. Panfilov,[2] S. Schlemmer,[1] Y. N. Kalugina,[3] A. Faure,[4,5] and A. van der Avoird[6,b)]
[1]*I. Physikalisches Institut, University of Cologne, Zülpicher Str. 77, 50937 Cologne, Germany*
[2]*Institute of Spectroscopy, Russian Academy of Sciences, Fizicheskaya Str. 5, 142190 Troitsk, Moscow, Russia*
[3]*Department of Optics and Spectroscopy, Tomsk State University, 36 Lenin av., 634050 Tomsk, Russia*
[4]*Université de Grenoble Alpes, IPAG, F-38000 Grenoble, France*
[5]*CNRS, IPAG, F-38000 Grenoble, France*
[6]*Theoretical Chemistry, Institute for Molecules and Materials, Radboud University Nijmegen, Heyendaalseweg 135, 6525 AJ Nijmegen, The Netherlands*

(Received 30 January 2015; accepted 5 March 2015; published online 19 March 2015)

The rotational spectrum of the van der Waals complex NH_3–CO has been measured with the intracavity OROTRON jet spectrometer in the frequency range of 112–139 GHz. Newly observed and assigned transitions belong to the $K = 0$–0, $K = 1$–1, $K = 1$–0, and $K = 2$–1 subbands correlating with the rotationless $(j_k)_{NH3} = 0_0$ ground state of free *ortho*-NH_3 and the $K = 0$–1 and $K = 2$–1 subbands correlating with the $(j_k)_{NH3} = 1_1$ ground state of free *para*-NH_3. The (approximate) quantum number K is the projection of the total angular momentum J on the intermolecular axis. Some of these transitions are continuations to higher J values of transition series observed previously [C. Xia *et al.*, Mol. Phys. **99**, 643 (2001)], the other transitions constitute newly detected subbands. The new data were analyzed together with the known millimeter-wave and microwave transitions in order to determine the molecular parameters of the *ortho*-NH_3–CO and *para*-NH_3–CO complexes. Accompanying *ab initio* calculations of the intermolecular potential energy surface (PES) of NH_3–CO has been carried out at the explicitly correlated coupled cluster level of theory with single, double, and perturbative triple excitations and an augmented correlation-consistent triple zeta basis set. The global minimum of the five-dimensional PES corresponds to an approximately T-shaped structure with the N atom closest to the CO subunit and binding energy $D_e = 359.21\ cm^{-1}$. The bound rovibrational levels of the NH_3–CO complex were calculated for total angular momentum $J = 0$–6 on this intermolecular potential surface and compared with the experimental results. The calculated dissociation energies D_0 are 210.43 and 218.66 cm^{-1} for *ortho*-NH_3–CO and *para*-NH_3–CO, respectively. © *2015 AIP Publishing LLC.* [http://dx.doi.org/10.1063/1.4915119]

I. INTRODUCTION

One of the reasons to investigate the NH_3–CO van der Waals complex concerns interpretation of the spectroscopic data coming from planetary atmospheres and the interstellar gas, because both ammonia and carbon monoxide are trace constituents in the solar system and they are present on ices in molecular clouds.[1,2] Another motivation to study the NH_3–CO system is its relevance to interactions between carbonyl and amine groups, which are important in many biological systems and required for modeling of the structures and dynamics of proteins. High resolution spectroscopy of van der Waals complexes together with *ab initio* calculations of the intermolecular potential is an efficient tool for reliable elucidation of the intermolecular forces, because bound states of the complexes are sensitive to the interaction potential.

The first spectroscopic observations of NH_3–CO have been carried out by Fraser *et al.*,[3] who observed the complex in the 6–21 GHz region using the technique of molecular beam electric resonance (MBER). They assigned a series of pure rotational transitions of the NH_3–CO complex (and less complete series of its ND_3, ND_2H, NDH_2, ^{13}CO isotopologues) in the $K = 0$ ground state. The ^{14}N quadrupole hyperfine structure of the observed transitions was resolved and analyzed, which provides the information that NH_3–CO is not hydrogen bonded and the N atom is closest to the CO subunit. Two further nearly degenerate pairs of series in the $K = 0$ and $K = 1$ excited states were detected. However, the exact nature of these excited states was not clear, and only limited information could be determined regarding the energy level pattern of NH_3–CO.

Subsequently, a more extensive study of NH_3–CO has been done by McKellar and co-workers,[4] where rovibrational (C–O stretching ≈2143 cm^{-1}) and pure rotational (76-106 GHz) transitions were measured in a pulsed jet supersonic expansion. The spectra included several subbands of infrared (IR) $v_{CO} = 1$–0 transitions, $K = 1$–0, $K = 0$–1, and $K = 2$–1, and a number of subbands of pure rotational millimeter-wave (MMW) transitions, $K = 0$–0, $K = 1$–1, $K = 1$–0, $K = 2$–1, in the $v_{CO} = 0$ ground state. In that work, the authors utilized the free internal rotation model to label the internal rotor states of NH_3–CO, where j_{NH3} and j_{CO} are quantum numbers for the in-

a)Electronic mail: surin@ph1.uni-koeln.de
b)Electronic mail: A.vanderAvoird@theochem.ru.nl

ternal rotations of the NH_3 and CO subunits. The total angular momentum J and its projection K on the intermolecular axis are the other useful quantum numbers.

As in the case of many other weakly bound complexes, for example, H_2–CO,[5,6] N_2–CO,[7,8] CH_4–CO,[9–11] the symmetry and nuclear spin modifications of the parent NH_3 molecule remain important in the NH_3–CO complex. Ammonia is a pyramidal symmetric top molecule with C_{3V} symmetry. Tunneling of the N atom through the plane of the H atoms causes an inversion splitting of the energy levels, with a magnitude of about 24 GHz in the ground vibrational state of free NH_3. Due to symmetry and nuclear spin statistics of the three equivalent protons in NH_3 all levels are separated into two distinct groups corresponding to complexes formed from *ortho*- or *para*-NH_3.[12] In spite of the higher multiplicity of the *ortho* nuclear spin states, the larger number of the *para* rotational levels results in approximately equal populations of the *ortho*- and *para*-NH_3 species. More details on the symmetry are given in Sec. IV. In the case of the NH_3–CO complex formed in a cold jet expansion, we need to consider only the lowest rotational energy level of each nuclear spin species of ammonia, namely, $(j_k)_{NH3} = 0_0$ for *ortho*-NH_3 and 1_1 for *para*-NH_3, where k is the projection of the NH_3 angular momentum j on the threefold symmetry axis.

Up to now, we have not been aware of any potential energy surface (PES) calculations for the NH_3–CO system. This paper presents the first *ab initio* PES of NH_3–CO carried out at the explicitly correlated coupled cluster level of theory with single, double, and perturbative triple excitations [CCSD(T)-F12a] and an augmented correlation-consistent triple zeta (aVTZ) basis set. The bound rotational levels of the NH_3–CO complex were calculated for total angular momentum $J = 0$–6 on this intermolecular potential surface and compared with the experimental results for both the *ortho*- and *para*-NH_3–CO spin modifications. Our new measurements of NH_3–CO extend the microwave (MW)[3] and MMW[4] transition series observed previously at lower frequencies to higher J values and reveal other newly detected subbands.

II. EXPERIMENTAL MEASUREMENTS AND EMPIRICAL ANALYSIS

A. Millimeter-wave experiment

MMW measurements in the frequency range of 112–139 GHz were made using the intracavity OROTRON jet spectrometer. The OROTRON spectrometer[13] combined with molecular jet expansion is a well-known technique[14] that has been used for more than ten years for the measurements of spectra of weakly bound complexes.

Briefly, the MMW generator OROTRON is placed in a vacuum chamber together with a supersonic jet. The free jet is injected into the OROTRON cavity perpendicularly to its axis. A high Q-factor ($\approx 10^4$) of the cavity results in 100 effective passes of the radiation through the jet. Absorption in the cavity causes changes of the electron current in the collector circuit of the OROTRON and is detected very sensitively by measuring these current changes. A small part of the MMW radiation is taken out from the cavity through coupling openings in a spherical mirror and mixed on a Schottky diode with the radiation of a MW synthesizer for frequency determination. The range of operation of the present OROTRON tube is 112–155 GHz with a few small gaps. A detailed description of the spectrometer has been published elsewhere.[14]

For the production of complexes, we used a gas mixture of 10% of NH_3 in CO at a backing pressure of 3-4 bars. The gas mixture was adiabatically expanded into the OROTRON cavity through a pulsed pin nozzle (General Valve, Series 9) with an opening diameter of 1 mm operated at a repetition rate of 8-12 Hz.

In addition to the NH_3–CO lines, many transitions of the CO dimer were also observed in the spectrum but most of them could be easily distinguished from the NH_3–CO lines due to the previous millimeter-wave survey of $(CO)_2$.[15]

B. Observed rotational spectrum

The previous IR and MMW studies[4] have shown that the spectrum and energy level pattern of *ortho*-NH_3–CO are relatively simple, closely resembling those of the rare gas–CO complexes. The situation for *para*-NH_3–CO was more complicated, and the observed states had K values differing by ±1 from those of the analogous *ortho*-NH_3–CO states. All observed *para*-NH_3–CO rotational lines revealed a small (a few MHz) doubling, not resolved in the IR spectrum.

The rotational energy levels of NH_3–CO with $K = 0$, 1, and 2 up to 25 cm^{-1} are shown in Fig. 1 for *ortho*-NH_3 (left diagram) and *para*-NH_3 (right diagram). Spectroscopic parity labels e ($\varepsilon = +1$) and f ($\varepsilon = -1$) are used to assign the parity p of individual levels according to the relation $p = \varepsilon\,(-1)^J$. The zero of energy for *ortho*-NH_3–CO is simply fixed at the lowest $J = 0$ level of the $K = 0$ ground state of the complex; the zero of energy for *para*-NH_3–CO is fixed at the $J = 0$ (virtual) level of the $K = 1$ ground state. The relative position of the *ortho* and *para*-NH_3–CO energy scales is determined by the zero-point levels of the *ortho* and *para* complexes obtained from the bound state calculations, see Sec. IV.

Using the reported data[4] for *ortho*-NH_3–CO, we predicted and found 14 new transitions with higher J values than accessed in the previous study. These include five $R(7)$-$R(11)$ transitions of the $K = 1$–0 subband, four $R(16)$-$R(19)$ transitions of the $K = 0$–0 subband, and five $R(16)$-$R(18)$ transitions of the $K = 1$–1 subband. Also, we were able to detect for the first time the $K = 2$–1 subband, which includes five $P_e(8)$-$P_e(12)$ and five $P_f(6)$-$P_f(10)$ transitions. A similar $K = 2$ state was observed in the IR spectrum of *ortho*-NH_3–CO for the excited $v_{CO} = 1$ state but not for the ground $v_{CO} = 0$ state.[4] Fig. 1 (left) shows the new $K = 1$–0 and $K = 2$–1 transitions with bold arrows and all previously observed transitions with thin arrows. The new $K = 0$–0 and $K = 1$–1 transitions connect levels located above 25 cm^{-1} and are not depicted on the diagram. The frequencies of all observed and assigned rotational lines for *ortho*-NH_3–CO are listed in Table I.

For *para*-NH_3–CO, we have detected at first four $R(5)$-$R(8)$ transitions of the $K = 2$–1 subband. They continue the transition series observed previously at lower frequencies[4] to higher J values. All observed $K = 2$–1 transitions exhibit a splitting of about 1 MHz in agreement with the trend from

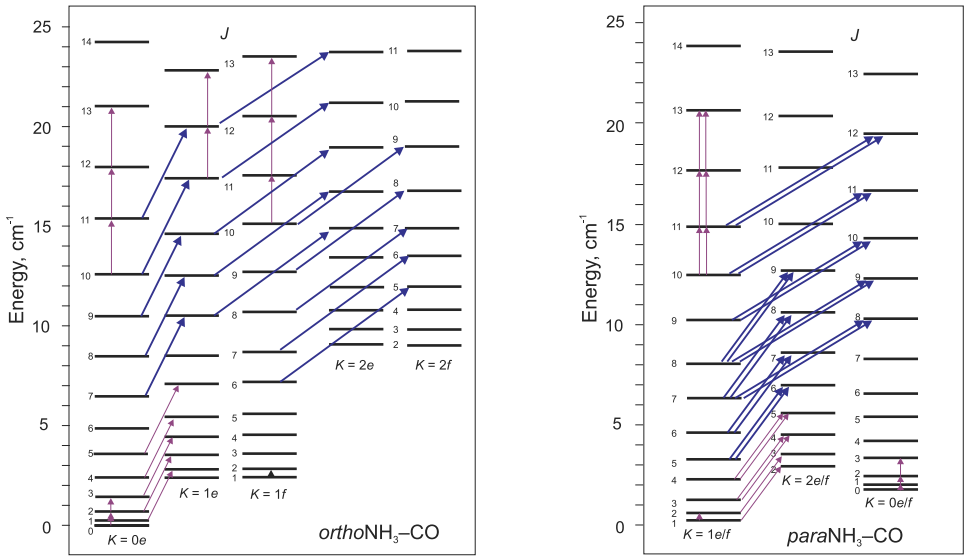

FIG. 1. Rotational energy levels and observed transitions of NH_3–CO. The relative position of the *ortho* and *para*-NH_3–CO energy scales is determined by the zero-point levels of the *ortho* and *para* complexes obtained from the bound state calculations, see Sec. IV. The new $\Delta K = \pm 1$ transitions are shown in bold (blue).

lower-J lines. Then carefully searching we were able to detect the new $K = 0$–1 subband and measured five $R(7)$-$R(11)$ transitions. This subband was not observed in the previous MMW study, although the rotational constants for the $K = 0$ state were estimated from the IR spectrum.[4] The new $K = 0$–1 lines exhibit a doubling with quite large 65-75 MHz splitting. At the beginning, we even overlooked these doublings and detected only one $K = 0(e)$–$1(e)$ subband. But then, analysing the results of the bound state calculations (Sec. IV) that predict the e/f splittings very accurately, the second $K = 0(f)$–$1(f)$ subband was found. All new and previously observed[3,4] rotational transitions are shown in Fig. 1 (right), and their frequencies and splittings are listed in Table II. The given frequencies from Refs. 3 and 4 represent the averaged values of two observed peaks (if they were resolved) for each transition.

The accuracy of frequency determination in the new measurements of both *ortho*-NH_3–CO and *para*-NH_3–CO is expected to be about 50 kHz. An exception is the position of the $K = 0$–0 $R(19)$ transition of *ortho*-NH_3–CO which could only be determined with a somewhat larger uncertainty of about 100 kHz. Fig. 2 shows an example of a recorded line, namely, the $R(6)$ $K = 2$–1 transition of *para*-NH_3–CO, demonstrating an e/f symmetry splitting of 0.86 MHz.

C. Empirical analysis

The transitions of NH_3–CO assigned in this work were fitted together with already known MW[3] and MMW data.[4] In the fitting procedure, the frequencies of the MMW and MW transitions were given weights of 1:50 according to the corresponding measurement accuracies. For *ortho*-NH_3–CO, we used an empirical energy expression in which each K-stack of levels was represented by a band origin σ plus a power series in $\left[J\,(J+1) - K^2\right]$, and an additional power series in $J\,(J+1)$ describing the asymmetry splitting

$$E_{total} = \sigma + B\left[J\,(J+1) - K^2\right] - D\left[J\,(J+1) - K^2\right]^2 + H\left[J\,(J+1) - K^2\right]^3 + L\left[J\,(J+1) - K^2\right]^4 + \Delta E_K, \quad (1)$$

$$\Delta E_K = \pm 1/2\left[bJ\,(J+1) + d(J\,(J+1))^2 + h(J\,(J+1))^3\right]. \quad (2)$$

In this expression, B is equivalent to $[(B+C)/2]$ and b is equivalent to $[(B-C)/2]$, where B and C are the nearly equal rotational constants of the complex, considered as a conventional near-prolate asymmetric rotor molecule. The asymmetry doubling term ΔE_K is equal to zero for $K = 0$, and starts at b for $K = 1$, at d for $K = 2$, etc.

The results of the fit for *ortho*-NH_3–CO are given in Table III together with the constants determined in the previous study.[4] The value of the root mean squared deviation $\sigma_{\rm fit}$ = 50 kHz for the MMW transitions is close to our experimental uncertainty. The parameters for the $K = 0$ and $K = 1$ states agree well with those obtained in Ref. 4, but in the present analysis, two more centrifugal distortion constants L and h for the $K = 1$ state had to be used because of the inclusion of higher-J transitions in the fit. The accurate molecular parameters for the $K = 2$ state were determined for the first time.

The asymmetry doubling term (2) was used only for the $K = 1$ and $K = 2$ states of *ortho*-NH_3–CO, but not for *para*-NH_3–CO, which was analysed as a symmetric top molecule (expression (1) with $\Delta E_K = 0$) following previous work.[4] It was also shown[4] that for the close-lying *para*-NH_3–CO states with $K = 0$ and 2, a Coriolis-type interaction should be introduced, linking levels of the same J value with a term given by

$$W = \beta\left\{\left[J(J+1)\right]\left[J\,(J+1) - 2\right]\right\}^{1/2}. \quad (3)$$

Here, β is a Coriolis-type interaction parameter representing a second order interaction. For all *para*-NH_3–CO transitions exhibiting some degree of doubling, the mean center frequencies were used in the fit analysis.

The spectroscopic constants obtained for the observed states of *para*-NH_3–CO are given in Table IV together with the constants determined in the previous study.[4] Overall there is a good agreement between the parameters, but their values for the $K = 0$ and $K = 2$ states are determined now with significantly better accuracy. The root mean squared deviation $\sigma_{\rm fit}$ = 150 kHz for the MMW transitions is larger than

TABLE I. Measured R-branch transitions for the *ortho*-NH_3–CO complex containing NH_3 in the $(j_k)_{NH3} = 0_0$ state. New values are given in bold.

Assignment		Frequency, MHz
$K = 1$–0; $j_{CO} = 1$–0	$R(1)$	77 357.037[a]
	$R(2)$	83 995.766[a]
	$R(3)$	90 521.435[a]
	$R(4)$	96 933.759[a]
	$R(5)$	103 233.241[a]
	$R(7)$	**115 498.157**
	$R(8)$	**121 467.514**
	$R(9)$	**127 331.395**
	$R(10)$	**133 092.993**
	$R(11)$	**138 755.753**
$K = 0$–0; $j_{CO} = 0$–0	$R(0)$	6 971.073[b]
	$R(1)$	13 939.502[b]
	$R(2)$	20 902.645[b]
	$R(10)$	76 097.934[a]
	$R(11)$	82 893.361[a]
	$R(12)$	89 656.786[a]
	$R(16)$	**116 333.267**
	$R(17)$	**122 893.771**
	$R(18)$	**129 404.586**
	$R(19)$	**135 863.150**
$K = 1(e)$–$1(e)$; $j_{CO} = 1$–1	$R(11)$	81 760.844[a]
	$R(12)$	88 461.611[a]
	$R(16)$	**114 962.465**
	$R(17)$	**121 498.817**
	$R(18)$	**127 994.410**
$K = 1(f)$–$1(f)$; $j_{CO} = 1$–1	$R(1)$	14 158[b]
	$R(10)$	77 350.861[a]
	$R(11)$	84 270.421[a]
	$R(12)$	91 159.894[a]
	$R(16)$	**118 358.501**
	$R(17)$	**125 052.750**
$K = 2(e)$–$1(e)$; $j_{CO} = 2$–1	$P(8)$	**138 521.998**
	$P(9)$	**132 617.887**
	$P(10)$	**126 854.034**
	$P(11)$	**121 236.214**
	$P(12)$	**115 770.536**
$K = 2(f)$–$1(f)$; $j_{CO} = 2$–1	$P(6)$	**146 163.057**
	$P(7)$	**138 473.112**
	$P(8)$	**130 695.433**
	$P(9)$	**122 835.080**
	$P(10)$	**114 897.369**

[a]Measured in Ref. 4.
[b]Hyperfine-free center frequencies of transitions measured in Ref. 3.

our experimental uncertainty of 50 kHz. Including higher order centrifugal parameters (L, β_J) improves the fit to some extent but also leads to a high correlation of the rotational parameters.

The authors of the previous MMW study[4] observed three "mystery" transitions not belonging to already presented series. These transitions exhibited some degree of doubling and were tentatively assigned to the $Q(9)$, $Q(10)$, and $Q(12)$ lines of the $K = 2$–1 subbands of *para*-NH_3–CO. We cannot confirm the proposed assignments because an inclusion of any of these transitions in our analysis significantly worsens the quality of the fit.

TABLE II. Measured R-branch transitions for the *para*-NH_3–CO complex containing NH_3 in the $(j_k)_{NH3} = 1_1$ state. New values are given in bold and represent the e–e/f–f components of the corresponding transition.

Assignment		Frequency, MHz	Splitting, MHz
$K = 2$–1; $j_{CO} = 1$–0	$R(1)$	82 858.148[a]	...
	$R(2)$	90 102.250[a]	...
	$R(3)$	97 494.452[a]	0.66[a]
	$R(4)$	105 056.346[a]	0.81[a]
	$R(5)$	**112 807.997/112 807.154**	0.84
	$R(6)$	**120 762.295/120 761.459**	0.84
	$R(7)$	**128 925.490/128 924.650**	0.84
	$R(8)$	**137 294.692/137 293.678**	1.01
$K = 1$–1; $j_{CO} = 0$–0	$R(1)$	13 780.4[b]	...
	$R(2)$	20 665.9[c]	3.6[c]
	$R(10)$	75 377.166[a]	1.988[a]
	$R(11)$	82 132.650[a]	2.119[a]
	$R(12)$	88 860.434[a]	2.245[a]
$K = 0$–0; $j_{CO} = 1$–1	$R(0)$	6 955.566[b]	...
	$R(1)$	13 899.339[b]	0.086[b]
	$R(2)$	20 820.4[b]	...
$K = 0$–1; $j_{CO} = 1$–0	$R(7)$	**111 864.185/111 787.790**	76.395
	$R(8)$	**118 506.310/118 432.746**	73.564
	$R(9)$	**125 027.440/124 956.454**	70.986
	$R(10)$	**131 427.718/131 359.295**	68.423
	$R(11)$	**137 710.853/137 644.626**	66.227

[a]Measured in Ref. 4; the center frequency and observed splitting were reported.
[b]Hyperfine-free center frequencies of transitions measured in Ref. 3.
[c]From Ref. 3 was not used in fit analysis because of unclear hfs/splitting structure.

III. CALCULATION OF THE POTENTIAL ENERGY SURFACE

A. Computational details

In this part of the work, we used the body-fixed (BF) coordinate system presented in Fig. 3. The origin of coordinate system 1 coincides with the center of mass of the NH_3 molecule and the z-axis is its threefold symmetry axis. The hydrogen atom labeled H′ of the NH_3 molecule lies in the xz-plane. The intermolecular vector $\boldsymbol{R}$ connects the centers of mass of

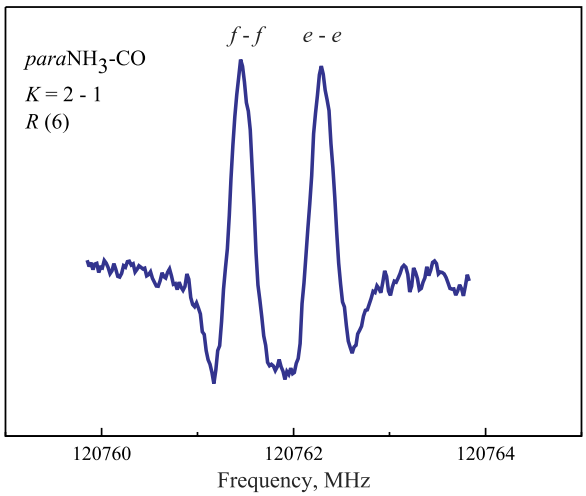

FIG. 2. Recording of the $K = 2$–1 $R(6)$ transition of *para*-NH_3–CO. Two peaks are due to small e/f symmetry splitting of the energy levels.

TABLE III. Molecular parameters for the *ortho*-NH_3–CO complex composed of NH_3 in the $(j_k)_{NH3} = 0_0$ state (all values in cm^{-1}).

		Present	Previous work (Ref. 4)
$K = 0$	σ	0.0	0.0
	B	0.116 272 60(22)	0.116 272 5(3)
	D	0.368 30(16) $\times 10^{-5}$	0.367 90(31) $\times 10^{-5}$
	H	−0.027 2(44) $\times 10^{-9}$	−0.056(11) $\times 10^{-9}$
$K = 1$	σ	2.242 530 8(17)	2.242 534(3)
	B	0.116 264 56(22)	0.116 265 7(7)
	D	0.305 26(16) $\times 10^{-5}$	0.305 5(6) $\times 10^{-5}$
	H	−0.182 0(60) $\times 10^{-9}$	−0.207(16) $\times 10^{-9}$
	L	−0.090 8(80) $\times 10^{-12}$	
	b	0.003 634 257(84)	0.003 637 4(10)
	d	−0.049 268(59) $\times 10^{-5}$	−0.051 9(31) $\times 10^{-5}$
	h	−0.702(11) $\times 10^{-10}$	
$K = 2$	σ	8.936 469 2(84)	[8.930][a]
	B	0.116 194 93(41)	0.116 238(19)
	D	0.244 54(52) $\times 10^{-5}$	[0.261 $\times 10^{-5}$][a]
	H	−0.498(22) $\times 10^{-9}$	
	d	−0.063 183(83) $\times 10^{-5}$	

[a]Estimated parameter.

the NH_3 and CO molecules. The angles θ_1 and φ_1 define the orientation of the vector $\boldsymbol{R}$ in body-fixed frame 1. The rotation of the CO molecule relative to frame 2, which is parallel to body-fixed frame 1, is defined by angles θ_2 and φ_2. Thus, the relative orientation of the NH_3 and CO molecules is described by a set of four angles $(\theta_1, \varphi_1, \theta_2, \varphi_2)$.

Ab initio calculations were performed for rigid interacting molecules with geometrical structures corresponding to the ground vibrational state: $r_{NH} = 1.916\, a_0$, $\angle(HNH) = 106.47°$,[16] and $r_{CO} = 2.137\, a_0$.[17] It was previously shown for other systems[18] that the use of the ground vibrational state geometry of the monomers for generation of the intermolecular potential gives a better agreement of theoretical predictions with experiment than the use of the equilibrium geometry.

TABLE IV. Molecular parameters for the *para*-NH_3–CO complex composed of NH_3 in the $(j_k)_{NH3} = 1_1$ state (all values in cm^{-1}).

		Present	Previous work (Ref. 4)
$K = 1$	σ	0.0	0.0
	B	0.114 929 9(33)	0.114 933 3(19)
	D	0.247 9(24) $\times 10^{-5}$	0.250 3(14) $\times 10^{-5}$
	H	−1.116(55) $\times 10^{-9}$	−1.060(33) $\times 10^{-9}$
$K = 0$	σ	1.757 532(89)	1.759 1(1)
	B	0.116 012 0(12)	0.116 005(5)
	D	0.323 1(160) $\times 10^{-5}$	0.03(26) $\times 10^{-5}$
	H	−6.986(140) $\times 10^{-9}$	
$K = 2$	σ	2.645 031 2(55)	2.645 011(20)
	B	0.116 723 4(33)	0.116 711(16)
	D	0.438 5(190) $\times 10^{-5}$	0.72(25) $\times 10^{-5}$
	H	−6.22(18) $\times 10^{-9}$	0.33(25) $\times 10^{-8}$
	β	0.002 354 1(180)	0.002 57(21)

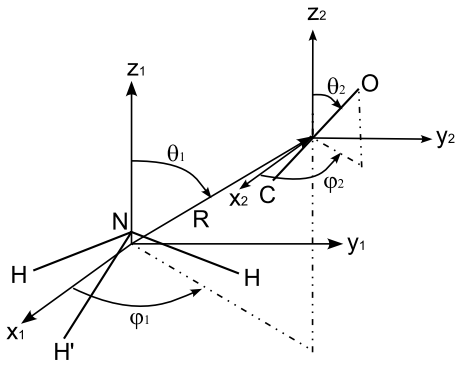

FIG. 3. Coordinate system of the NH_3–CO system.

It is well known that for the description of noncovalent interactions between molecules that can be described by a single electronic configuration, the golden standard is the CCSD(T) level in combination with a Complete Basis Set (CBS) limit. Thus, our purpose is to obtain the interaction potential of NH_3–CO close to this level. First, we have performed some tests to find the most suitable method and basis set (computationally feasible and accurate). The performance of different basis sets, including results extrapolated to the CBS limit (extrapolation scheme of Peterson *et al.*[19]), at the CCSD(T) level is illustrated in Fig. 4. We also show the results obtained at the explicitly correlated CCSD(T)-F12a[20] and a medium-sized basis set. It was previously shown [21–23] that the CCSD(T)-F12 method can provide accurate spectroscopic data for bimolecular complexes. It is seen in Fig. 4 that the results close to the reference CCSD(T)/CBS method are obtained by the CCSD(T)-F12a method with an aVTZ basis.[24] Hence, we calculated the PES of the NH_3–CO complex in its ground electronic state at the CCSD(T)-F12a level of theory with the aVTZ basis using the MOLPRO 2010 package.[25] The exponent β in the correlation factor F_{12} was set to 1.3. We used the standard auxiliary basis sets and density fitting functions[26,27] (CABS(OptRI) basis sets). The basis set superposition error (BSSE) correction was taken into account with the Boys and Bernardi counterpoise scheme[28] and the interaction potential is given by

$$V(R,\theta_1,\varphi_1,\theta_2,\varphi_2) = E_{NH3-CO}(R,\theta_1,\varphi_1,\theta_2,\varphi_2) - E_{NH3}(R,\theta_1,\varphi_1,\theta_2,\varphi_2) - E_{CO}(R,\theta_1,\varphi_1,\theta_2,\varphi_2),$$

where the energies of the NH_3 and CO monomers are calculated in the full basis of the complex.

The F12 triple energy correction in MOLPRO is not taken into account directly, but with a scaling term,[20] which leads to a slight size inconsistency. This size inconsistency was corrected for by subtracting from $V(R,\theta_1,\varphi_1,\theta_2,\varphi_2)$ the asymptotic interaction energy at $R = 1000\, a_0$, which is 6.57 cm^{-1} for all relative orientations.

The PES calculations were carried out for a large random grid of angular orientations, i.e., for each value of the intermolecular separations R, the energies of about 3000 random relative orientations were calculated. The R-values were varied from 4.5 to 30 a_0 with 31 radial grid points for each angular orientation. The advantage of using random angular grids is

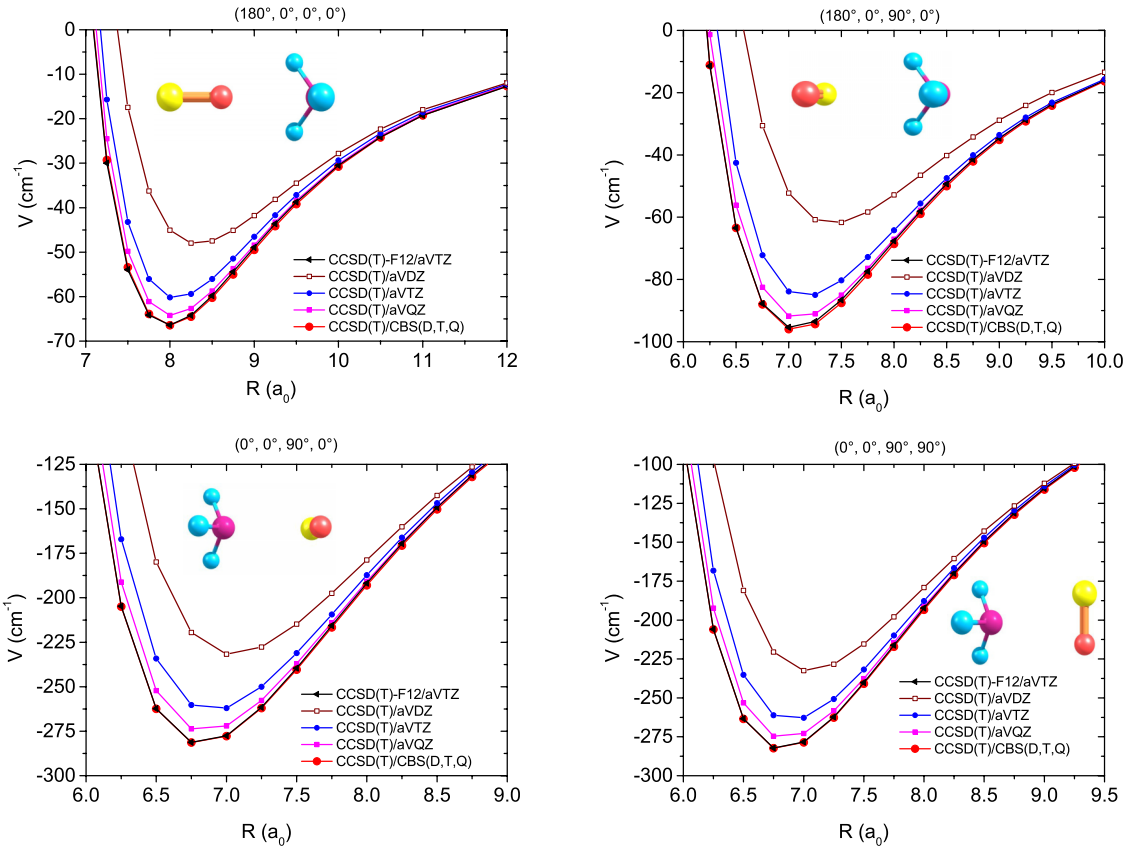

FIG. 4. NH_3–CO interaction energies for different basis sets and methods as a function of the intermolecular distance for selected angular orientations.

that they allow an estimate of the accuracy of each expansion coefficients,[29] as illustrated below.

B. Analytical fit

The analytical expansion for a symmetric-top-linear molecule system can be written as

$$V(R,\theta_1,\varphi_1,\theta_2,\varphi_2) = \sum v_{l_1 m_1 l_2 l}(R)\, t_{l_1 m_1 l_2 l}(\theta_1,\varphi_1,\theta_2,\varphi_2),$$

where the five body-fixed coordinates (R, θ_1, φ_1, θ_2, φ_2) are defined in Fig. 3 and where the functions $t_{l_1 m_1 l_2 l}$ (θ_1, φ_1, θ_2, φ_2) are explicitly given by Phillips *et al.*[30] and by Valiron *et al.*,[31] The indices l_1, l_2, and l refer to the tensor rank of the dependence of the potential on the NH_3 orientation, the CO orientation, and the collision vector orientation, respectively. As detailed in Phillips *et al.*,[30] a phased sum over $\pm m_1$ guarantees that the functions are symmetric on reflection in the NH_3 molecule xz-plane. In the rigid rotor approximation, the C_{3V} symmetry of NH_3 further requires that m_1 is a multiple of 3. We selected the maximum tensor ranks in order to include all anisotropies up to $l_1 = 10$, $l_2 = 10$, and $l = 20$, resulting in 2111 expansion functions. We then selected iteratively all significant terms, at each intermolecular separation R, using the following procedure: we started the fit with a minimal selection limited to the single function t_{0000} and evaluated the 2110 remaining terms by random quadrature. All terms above a Monte Carlo error estimator (defined by Rist and Faure[29]) were then selected and added to t_{0000}, providing a new starting expansion. The process was iterated until convergence.

The final set, obtained by merging the selected sets at all distances R, was composed of 250 expansion functions, including anisotropies up to $l_1 = 10$ (with $m_1 = 0, 3, 6$), $l_2 = 10$, and $l = 18$. The root mean square residual was found to be lower than 1 cm^{-1} in the long-range and van der Waals well region of the interaction ($R > 6$ bohr). In this part of the PES, the mean error in the expansion coefficients $v_{l_1 m_1 l_2 l}(R)$ was also found to be smaller than 1 cm^{-1}. A cubic spline interpolation of each coefficient $v_{l_1 m_1 l_2 l}(R)$ was finally employed over the whole intermolecular distance range ($R = 4.5 - 30$ bohr) and it was smoothly connected to standard extrapolations (exponential and inverse power laws at short and long range, respectively) in order to provide continuous radial expansion coefficients suitable for the bound states calculations presented below. Details on the switch function are given by Valiron *et al.*,[31] see their Eq. (10).

The global minimum of the five-dimensional (5D) PES corresponds to the structure with $\theta_1 = 38.1°$, $\varphi_1 = 0°$, $\theta_2 = 23.2°$, $\varphi_2 = 180°$, and $R = 6.85\, a_0$ with binding energy $D_e = 359.21$ cm^{-1}.

In Fig. 5, we present the 2D cuts (other variables are fixed at their equilibrium values corresponding to the global minimum) of the 5D PES of the NH_3–CO complex. It is noticeable that the potential depends strongly on the orientations of both monomers.

IV. BOUND STATES CALCULATION

The method used to calculate the rovibrational levels of NH_3–CO is described in Ref. 32, where it was applied to

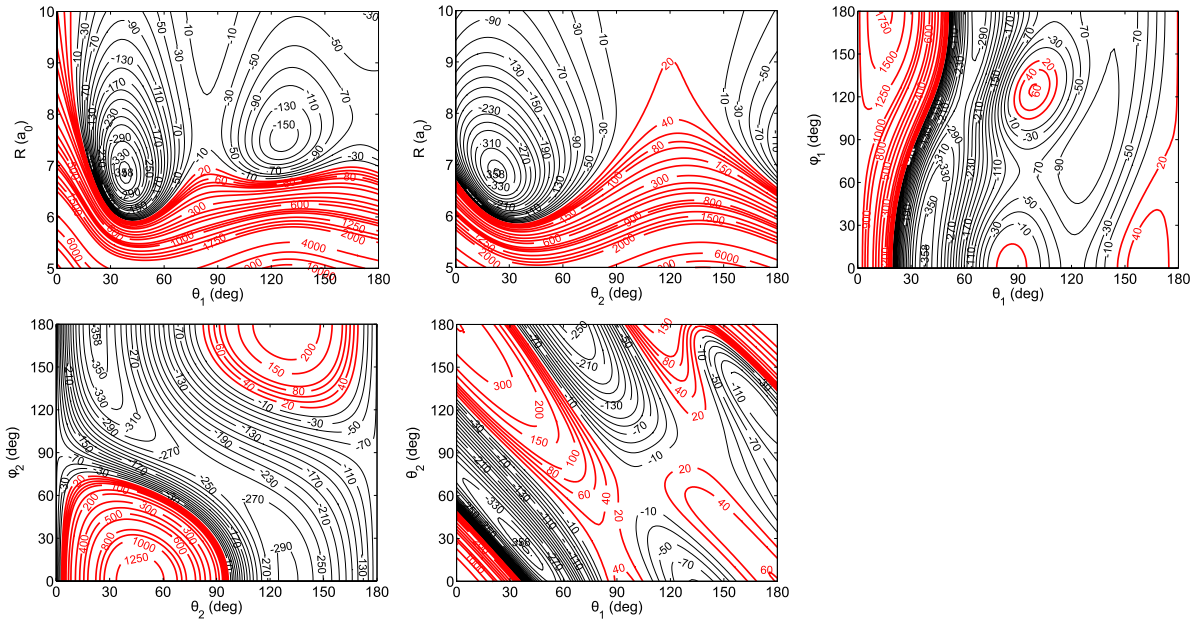

FIG. 5. Potential energy cuts of the 5D PES: two coordinates are changing while others are fixed at their equilibrium values corresponding to the global minimum. Energy contour labels are in cm^{-1}.

H_2O–H_2. It is based on a general computational method[33] developed for weakly bound molecular dimers with large amplitude internal motions and is similar to a coupled-channel scattering approach. For all details on the form of the Hamiltonian and the basis in BF coordinates, etc., we refer to Ref. 34. NH_3 is an oblate symmetric rotor; we used the ground state experimental values for its rotational constants: $A_0 = B_0 = 9.9402\ cm^{-1}$, $C_0 = 6.3044\ cm^{-1}$, and the measured value of $B_0 = 1.922\,53\ cm^{-1}$ for CO. The atomic masses are 1.007 825 u for H, 14.003 074 u for ^{14}N, 12 for ^{12}C, and 15.994 915 u for ^{16}O. The grid in the discrete variable representation (DVR) for the intermolecular center-of-mass distance R contained 162 equidistant points ranging from $R = 4.5$ to 20 a_0. We used a radial basis of 20 functions contracted in the same way as in Ref. 32. The angular basis of symmetric rotor functions—Wigner D-functions[34]—and spherical harmonics for the hindered rotations of NH_3 and CO, respectively, was truncated to internal rotor quantum numbers $j_{NH3} \le 8$ and $j_{CO} \le 14$. These values are sufficient to converge the bound levels of the complex to better than $0.01\ cm^{-1}$, but the energy differences between the levels are converged much more accurately. Also, the overall rotation of the dimer was described with Wigner D-functions.

An additional motion in the NH_3–CO complex is the umbrella inversion tunneling of the NH_3 monomer, with a level splitting of $0.7934\ cm^{-1}$ in the free monomer. As discussed in Sec. V, this tunneling motion is nearly quenched in the dimer states and the corresponding splittings become very small. The potential described in Sec. III does not include this umbrella inversion motion, so we applied a two-state model, which was also used and tested in previous work on NH_3–He[35,36] and NH_3–Ar.[37] This model assumes that the NH_3 inversion tunneling motion occurs between two structures, umbrella up and umbrella down, with the umbrella angle corresponding to the equilibrium value in free NH_3. The potential was only calculated for one of these structures; its value for the umbrella-inverted structure is obtained from a symmetry relation obeyed by the expansion coefficients described in Sec. III. The two-state model implies that the basis for the rovibrational states of the complex is extended with two NH_3 inversion tunneling states that are the plus and minus combinations of the two localized umbrella states. When the NH_3 tunneling in the complex is quenched by the interaction with CO, these states become more or less localized.

The permutation-inversion (PI) or molecular symmetry[38] group $G_{12} \equiv D_{3h}(M)$ of NH_3–CO is the same as for NH_3–He[35,36] and NH_3–Ar.[37] The irreducible representations (irreps) of this symmetry group are A_1', A_1'', A_2', A_2'', and E', E'', with states belonging to these irreps having nuclear spin statistical weights[38] of 0, 0, 12, 12, and 6, 6, respectively. Since the nuclear spin functions do not change during the measurements, these symmetries are conserved, and the Pauli-forbidden states of A_1 symmetry cannot be observed. The rovibrational wave functions of the A_1 and A_2 (*ortho*) states are composed of NH_3 monomer functions with $k_{NH3} = 0$ (modulo 3), while those of E-symmetry (*para*) states have $k_{NH3} = \pm 1$ (modulo 3). The quantum number k_{NH3} is the projection of the NH_3 monomer angular momentum j_{NH3} on its threefold symmetry axis. Each rovibrational state of NH_3–CO has two NH_3 inversion tunneling components, with A_1' and A_2'' symmetries, A_1'' and A_2' symmetries, or E' and E'' symmetries. Since the states of A_1 symmetry have nuclear spin weight 0, the inversion tunneling splittings cannot be observed for the *ortho* states of NH_3–CO. They are visible only in the spectra for the *para* states of E symmetry.

The total angular momentum J and the parity $p = \pm 1$ under inversion are exact quantum numbers. In our analysis of the rovibrational states, we use the spectroscopic parity ε, which is related to the inversion parity by $p = \varepsilon(-1)^J$. We follow the convention to label states of even/odd spectroscopic parity by e/f. An approximate quantum number that is important to understand the nature of the rovibrational states

is the projection K of the total angular momentum J on the intermolecular axis $\boldsymbol{R}$. We use the absolute value of K as a label and distinguish the states with $K > 0$ by their parity e/f. Calculations have been performed for J values from 0 to 6 for all symmetries.

We found that the ground level of *ortho*-NH_3–CO corresponds to $K = 0$, $J = 0$ with an energy of -209.63 cm^{-1} relative to the separated *ortho*-NH_3 ($j_k = 0_{0+}$) and CO ($j = 0$) monomers. The even (+) inversion tunneling component of the $j_k = 0_0$ ground state of *ortho*-NH_3 is Pauli-forbidden, however, and since the odd (−) component is 0.79 cm^{-1} higher in energy, the dissociation energy of *ortho*-NH_3–CO is $D_0 = 210.43$ cm^{-1}. The ground level of *para*-NH_3–CO has $K = 1$, $J = 1$ and was calculated at -202.32 cm^{-1}. Since the ground ($j_k = 1_{1+}$) state of free *para*-NH_3 has an energy of 16.33 cm^{-1}, the dissociation energy D_0 of *para*-NH_3–CO is 218.66 cm^{-1}. Thus, D_0 is slightly larger for *para*-NH_3–CO than for *ortho*-NH_3–CO. We note, furthermore, that a significant fraction of the binding energy $D_e = 359.21$ cm^{-1} goes into the zero-point energy associated with the intermolecular vibrations and internal rotations.

V. DISCUSSION

The calculated positions of the lower states (<10 cm^{-1}) with $K = 0$, 1, 2, 3 of the NH_3–CO complex that links the subbands detected or searched for in the present work are shown in Fig. 6. The zeros of energies for *ortho*-NH_3–CO and *para*-NH_3–CO are fixed at their lowest levels. At first sight, one may think that the levels in this picture correspond to a free internal rotor quantum number j_{CO} increasing from 0 to 1 to 2 and that the observed subbands correlate with $\Delta j_{CO} = 1$. Such a free internal rotor interpretation is not valid, however, since analysis of the calculated wave functions shows that the j_{CO} values are strongly mixed by the anisotropic interaction potential. According to the bound state calculations, the zero of the *para*-NH_3–CO energy scale is about 7 cm^{-1} higher than the zero of the *ortho*-NH_3–CO scale. This number is about half of the value estimated in Ref. 4 assuming free rotation of the NH_3 unit in the complex.

It was established in the previous experimental study[4] and confirmed here by the *ab initio* calculations that *ortho*-NH_3–CO has a ground state with $K = 0$, while the ground state of *para*-NH_3–CO is a $K = 1$ state (see Fig. 6). This is related to the fact that the *para*-NH_3–CO states begin with $j_{NH3} = k_{NH3} = 1$ and that the lowest energy orientation of *para*-NH_3 in the complex has a Π configuration ($K = 1$) with the resultant angular momentum of NH_3 oriented parallel to the intermolecular axis of the complex. By contrast, the *ortho*-NH_3–CO states begin with $j_{NH3} = k_{NH3} = 0$, and a Σ configuration ($K = 0$) has the lowest energy.

Another difference between the two nuclear spin species, as can be seen from Fig. 6, is that the e/f splitting of the $K = 1$ and $K = 2$ states is much larger for *ortho*-NH_3–CO than for *para*-NH_3–CO. In the theory, this e/f splitting originates from the Coriolis coupling with $\Delta K = \pm 1$ between the $K = 0$ levels and the levels with $K > 0$, for $K = 1$ directly, for $K = 2$ indirectly through $K = 1$, etc. This explains also why the e/f splittings decrease rapidly with increasing K. For *ortho*-NH_3–CO, this mixing occurs only for the e state, not for the f state, because the $K = 0$ level has parity e. This causes the splitting, because the energy of the $K = 1$ level of parity e is changed by the mixing, while the energy of the level of parity f does not change. For *para*-NH_3–CO, the $K = 0$ level occurs with both parities e and f. And the $K = 1$ levels of e and f parity mix by almost the same amount to the corresponding $K = 0$ levels. Hence, there is only a very small splitting between the e and f levels. The reason why for *para*-NH_3–CO

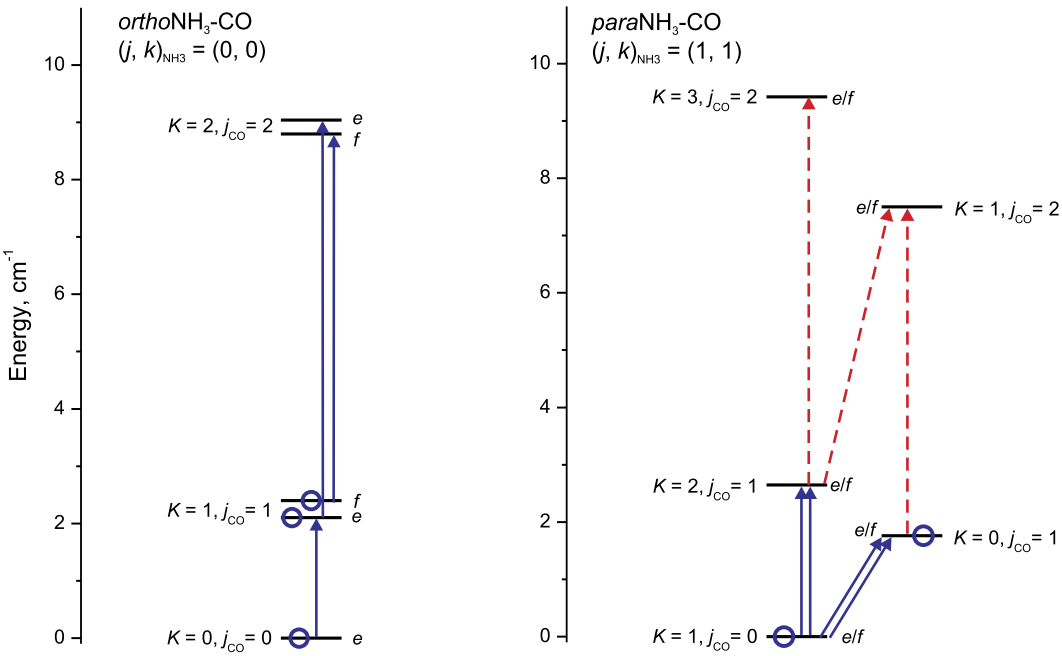

FIG. 6. Calculated energies of the levels with $K = 0$, 1, 2, 3 that link the subbands detected (blue solid lines) or searched for (red dashed lines) in the present work. Individual transitions in these subbands are shown in Fig. 1. Circles mean that *end-over-end* rotational transitions were observed within these states.

(E symmetry) both parities e and f occur for $K = 0$ is because $k_{NH3} = 1$ for *para*-NH_3. Inversion, which distinguishes e/f (actually +/−) states, produces two low-lying states, with $k_{NH3} = +1$ and −1. Their plus and minus combinations are the +/−(or e/f) states. While for *ortho*-NH_3–CO, the lowest state has $k_{NH3} = 0$, so that for $K = 0$, only the e state occurs.

The inversion tunneling motion of ammonia is nearly quenched for all states in *para*-NH_3–CO. Although the calculated splitting of the $K = 0$ levels is about 100 times larger than the splitting of the $K = 1$ levels, its absolute value of ~80 MHz (~0.003 cm^{-1}) is significantly lower than the inversion splitting in free NH_3 (23.9 GHz or 0.79 cm^{-1}). Qualitatively, this picture is the same as observed and calculated for the NH_3–Ar complex,[37,39] where the inversion motion of ammonia is hardly affected in the $K = 0$ states, while it is nearly quenched in the $K = 1$ states. The reason that the inversion splittings are much smaller in NH_3–CO than in NH_3–Ar is that the anisotropy of the intermolecular potential is much larger when NH_3 interacts with CO than when it interacts with Ar.

For both spin modifications, all three lowest stacks with $K = 0$, 1, 2 shown in Fig. 6 are now well characterized by MW and MMW spectroscopies. In Table V and Table VI, the experimentally determined energy levels of *ortho*-NH_3–CO and *para*-NH_3–CO are compared with the results of bound state calculations. The theory predicts very accurately the origins of the observed K-stacks as can be seen from comparison of their lowest-J levels, but the (Observation—Calculation) deviations grow rapidly with increasing total angular momentum and amount to about +0.1 cm^{-1} at the maximum calculated value of $J = 6$. This indicates that the end-over-end rotational constant $[(B + C)/2]$ from the calculations is too small by about 2%, which corresponds to the average distance R being too large by about 1%. The reason could be that the minimum in the intermolecular potential occurs slightly too far outwards. Calculations with larger basis sets did not produce a shift of the minimum, however. A possible reason for the observed difference may be that our calculations use the rigid monomer model, which may be somewhat inaccurate especially for NH_3. The e/f splitting for *ortho*-NH_3–CO levels is reproduced by theory with an accuracy better than 0.006 cm^{-1} for the $K = 1$ state and better than 0.0001 cm^{-1} for the $K = 2$ state. The e/f splitting for *para*-NH_3–CO levels cannot be determined directly from the experiment, because no transitions between e and f levels were detected. However, the observed splittings for the *para*-NH_3–CO transitions given in Table II are also very well reproduced by theory, with deviations less than 10 MHz (0.0003 cm^{-1}) for the $K = 0$–1 subband and less than 1 MHz (0.000 03 cm^{-1}) for the $K = 2$–1 subband.

Unfortunately, we were unable to detect the expected subbands for transitions to the $K = 3$ state and the second $K = 1$ (upper) state (shown by dashed lines in red in Fig. 6). The corresponding P-branch transitions were predicted by theory to be in the range of our spectrometer starting from $J = 5$ for the $K = 1$–2, $J = 7$ for the $K = 1$–0, and $J = 8$ for the $K = 3$–2 subbands. Similar $K = 3$ and $K = 1$ (upper) stacks of *para*-NH_3–CO were observed in the IR work[4] for the excited $v_{CO} = 1$ state. The authors also estimated the rotational constants (but not directly from experiment) for $K = 3$

TABLE V. Calculated (*ab initio*) and experimental energy levels of the *ortho*-NH_3–CO complex.

State	J	Calculation, cm^{-1}	Observation, cm^{-1}	O-C, cm^{-1}
$K = 0$ (e)	0	0.000 00	0.000 00	0.000
	1	0.227 29	0.232 53	0.005
	2	0.681 79	0.697 50	0.016
	3	1.363 33	1.394 74	0.031
	4	2.271 67	2.323 98	0.052
	5	3.406 47	3.484 86	0.078
	6	4.767 32	4.876 95	0.110
$K = 1$ (e)	1	2.361 54	2.355 16	−0.006
	2	2.809 05	2.812 88	0.004
	3	3.480 16	3.499 30	0.019
	4	4.374 67	4.414 21	0.040
	5	5.492 35	5.557 34	0.065
	6	6.832 86	6.928 35	0.095
$K = 1$ (f)	1	2.368 53	2.362 43	−0.006
	2	2.830 01	2.834 67	0.005
	3	3.522 04	3.542 84	0.021
	4	4.444 40	4.486 70	0.042
	5	5.596 80	5.665 92	0.069
	6	6.978 85	7.080 12	0.101
$K = 2$ (e)	2	9.199 81	9.168 86	−0.031
	3	9.881 05	9.865 92	−0.015
	4	10.789 15	10.795 09	0.006
	5	11.923 96	11.956 16	0.032
	6	13.285 26	13.348 88	0.064
$K = 2$ (f)	2	9.168 86	9.168 84	−0.031
	3	9.865 92	9.865 83	−0.015
	4	10.795 09	10.794 83	0.006
	5	11.956 16	11.955 59	0.032
	6	13.348 88	13.347 76	0.063

TABLE VI. Calculated (*ab initio*) and experimental energy levels of the *para*-NH_3–CO complex (averaged values are given for the e/f components).

State	J	Calculation, cm^{-1}	Observation, cm^{-1}	O-C, cm^{-1}
$K = 1$	1	0.112 41	0.114 93	0.003
	2	0.562 02	0.574 59	0.013
	3	1.236 29	1.263 93	0.028
	4	2.135 03	2.182 77	0.048
	5	3.258 02	3.330 86	0.073
	6	4.604 95	4.707 89	0.103
$K = 0$	0	1.760 03	1.758 95	−0.001
	1	1.986 68	1.990 96	0.004
	2	2.439 65	2.454 60	0.015
	3	3.118 26	3.149 09	0.031
	4	4.021 61	4.073 40	0.052
	5	5.148 58	5.226 26	0.078
	6	6.498 00	6.606 36	0.108
$K = 2$	2	2.886 51	2.878 77	−0.008
	3	3.571 76	3.580 08	0.008
	4	4.486 16	4.516 00	0.030
	5	5.630 17	5.687 07	0.057
	6	7.004 19	7.093 71	0.090

in the ground $v_{CO} = 0$ state. Using these constants,[4] the expected frequencies for the $K = 3$–2 transitions deviate by more than 10 GHz, i.e., 0.3 cm^{-1}, from the theoretically predicted values. It makes the search range of the $K = 3$–2 subband very uncertain. As mentioned above, the inaccuracy of the theoretical values can be relatively large for such higher J values.

VI. CONCLUSIONS

This paper describes the new observation of the millimeter-wave spectrum of the NH_3–CO complex and calculation of the rovibrational bound states on a 5D intermolecular potential surface obtained through high-level *ab initio* calculations. The observed transitions were assigned to the $K = 0$–0, $K = 1$–1, $K = 1$–0, and $K = 2$–1 subbands correlating with the rotationless $(j_k)_{NH3} = 0_0$ state (A symmetry) of free *ortho*-NH_3, and the $K = 0$–1 and $K = 2$–1 subbands correlating with the $(j_k)_{NH3} = 1_1$ state (E symmetry) of free *para*-NH_3. These measurements were included in a simultaneous fit together with the previous data to determine an improved set of empirical molecular parameters for both *ortho*-NH_3–CO and *para*-NH_3–CO. All bound rovibrational levels of the two nuclear spin species were computed for total angular momentum $J = 0$–6.

It was found from the calculations that the global minimum of the 5D PES corresponds to a structure with intermolecular separation $R = 6.85\,a_0$ and binding energy $D_e = 359.21$ cm^{-1}. The C_3 axis of the NH_3 subunit is oriented at an angle of 38.1° with respect to the axis connecting the centers of mass of the two subunits and the N atom is closest to the CO subunit. A significant fraction of the binding energy goes into the zero-point energy associated with the intermolecular vibrations and internal rotations: the dissociation energies D_0 are 210.43 and 218.66 cm^{-1} for *ortho*-NH_3–CO and *para*-NH_3–CO, respectively.

The computed energy levels were compared with the rotational spectra measured earlier and in the present work. We found a good agreement with the experiment for all detected stacks although we noted a systematic increase of the rotational energy differences with increasing J, which indicates that the calculated end-over-end rotational constant of the complex is too small by about 2%. The reason for the latter deviation may be the use of a rigid monomer model, especially for NH_3.

Finally, we can conclude that the present results provide a considerable amount of new information, both experimental and theoretical, which elucidate the intermolecular interactions and dynamics in the NH_3–CO system.

ACKNOWLEDGMENTS

This work was supported by Deutsche Forschungsgemeinschaft (DFG) through research Grant No. SU 579/1-2 and by Russian Foundation for Basic Research through Grant No. 15-03-09333. A.P. acknowledges support by DFG via SFB 956. Y.K. acknowledges the support of Russian Foundation for Basic Research (Project No. 13-05-00751). *Ab initio* calculations were carried out using HPC resources of Skif-Cyberia (Tomsk State University).

[1] *Solar System Ices*, edited by B. Schmitt, C. De Bergh, and M. Festou (Kluwer, Dordrecht, 1998).
[2] L. J. Allamandola, M. P. Bernstein, S. A. Sandford, and R. L. Walker, Space Sci. Rev. **90**, 219 (1999).
[3] G. T. Fraser, D. D. Nelson, Jr., K. I. Peterson, and W. Klemperer, J. Chem. Phys. **84**, 2472 (1986).
[4] C. Xia, K. A. Walker, and A. R. W. McKellar, Mol. Phys. **99**, 643 (2001).
[5] A. R. W. McKellar, J. Chem. Phys. **108**, 1811 (1998).
[6] A. V. Potapov, L. A. Surin, V. A. Panfilov, B. S. Dumesh, T. F. Giesen, S. Schlemmer, P. L. Raston, and W. Jäger, Astrophys. J. **703**, 2108 (2009).
[7] M. Rezaei, K. H. Michaelian, N. Moazzen-Ahmadi, and A. R. W. McKellar, J. Phys. Chem. A **117**, 13752 (2013).
[8] L. Surin, A. Potapov, H. S. P. Müller, and S. Schlemmer, J. Mol. Spectrosc. **307**, 54 (2015).
[9] C. Xia, K. A. Walker, and A. R. W. McKellar, J. Chem. Phys. **114**, 4824 (2001).
[10] Y. Liu and W. Jäger, J. Chem. Phys. **121**, 6240 (2004).
[11] A. V. Potapov, A. A. Dolgov, V. A. Panfilov, L. A. Surin, and S. Schlemmer, J. Mol. Spectrosc. **268**, 112 (2011).
[12] W. Gordy and R. L. Cook, *Microwave Molecular Spectra*, 3rd ed. (John Wiley & Sons Inc., 1984).
[13] B. S. Dumesh and L. A. Surin, Rev. Sci. Instrum. **67**, 3458 (1996).
[14] L. A. Surin, B. S. Dumesh, F. Lewen, D. A. Roth, V. P. Kostromin, F. S. Rusin, G. Winnewisser, and I. Pak, Rev. Sci. Instrum. **72**, 2535 (2001).
[15] L. A. Surin, D. N. Furzikov, T. F. Giesen, S. Schlemmer, G. Winnewisser, V. A. Panfilov, B. S. Dumesh, G. W. M. Vissers, and A. van der Avoird, J. Phys. Chem. A **111**, 12238 (2007).
[16] G. Herzberg, *Infrared and Raman Spectra of Polyatomic Molecules, Molecular Spectra and Molecular Structure Vol. 2* (Van Nostrand, New York, 1945), p. 632.
[17] K. P. Huber and G. Herzberg, *Molecular Spectra and Molecular Structure. IV. Constants of Diatomic Molecules* (Van Nostrand Reinhold, New York, 1979).
[18] P. Jankowski and K. Szalewicz, J. Chem. Phys. **123**, 104301 (2005).
[19] K. A. Peterson, D. E. Woon, and T. H. Dunning, Jr., J. Chem. Phys. **100**, 7410 (1994).
[20] H.-J. W. G. Knizia and T. B. Adler, J. Chem. Phys. **130**, 054104 (2009).
[21] Y. Ajili, K. Hammami, N. E. Jaidane, M. Lanza, Y. N. Kalugina, F. Lique, and M. Hochlaf, Phys. Chem. Chem. Phys. **15**, 10062 (2013).
[22] F. Lique, J. Klos, and M. Hochlaf, Phys. Chem. Chem. Phys. **12**, 15672 (2010).
[23] Y. Kalugina, I. Buryak, Y. Ajili, A. Vigasin, N.-E. Jaidane, and M. Hochlaf, J. Chem. Phys. **140**, 234310 (2014).
[24] T. H. Dunning, J. Chem. Phys. **90**, 1007 (1989).
[25] H.-J. Werner, P. J. Knowles, G. Knizia, F. R. Manby, M. Schütz *et al.*, MOLPRO, version 2010.1, a package of *ab initio* programs, 2010, see http://www.molpro.net.
[26] W. Klopper, Mol. Phys. **99**, 481 (2001).
[27] F. Weigend, A. Köhn, and C. Hättig, J. Chem. Phys. **116**, 3175 (2002).
[28] S. F. Boys and F. Bernardi, Mol. Phys. **19**, 553 (1970).
[29] C. Rist and A. Faure, J. Math. Chem. **50**, 588 (2011).
[30] T. R. Phillips, S. Maluendes, A. D. McLean, and S. Green, J. Chem. Phys. **101**, 5824 (1994).
[31] P. Valiron, M. Wernli, A. Faure, L. Wiesenfeld, C. Rist, S. Kedžuch, and J. Noga, J. Chem. Phys. **129**, 134306 (2008).
[32] A. van der Avoird and D. J. Nesbitt, J. Chem. Phys. **134**, 044314 (2011).
[33] G. C. Groenenboom, P. E. S. Wormer, A. van der Avoird, E. M. Mas, R. Bukowski, and K. Szalewicz, J. Chem. Phys. **113**, 6702 (2000).
[34] D. M. Brink and G. R. Satchler, *Angular Momentum*, 3rd ed. (Clarendon, Oxford, 1993).
[35] K. B. Gubbels, S. Y. T. van de Meerakker, G. C. Groenenboom, G. Meijer, and A. van der Avoird, J. Chem. Phys. **136**, 074301 (2012).
[36] O. Tkac, A. Kumar Saha, J. Onvlee, C.-H. Yang, G. Sarma, C. Bishwarkarma, S. Y. T. van de Meerakker, A. van der Avoird, D. H. Parker, and A. J. Orr-Ewing, Phys. Chem. Chem. Phys. **16**, 477 (2014).
[37] J. Loreau, J. Liévin, Y. Scribano, and A. van der Avoird, J. Chem. Phys. **141**, 224303 (2014).
[38] P. R. Bunker and P. Jensen, *Molecular Symmetry and Spectroscopy*, 2nd ed. (NRC Research Press, Ottawa, Canada, 1998).
[39] E. Zwart, H. Linnartz, W. Leo Meerts, G. T. Fraser, D. D. Nelson, Jr., and W. Klemperer, J. Chem. Phys. **95**, 793 (1991).